AD-A154 886 GUIDED-MODE LAUNCHING IN A SLAB WAVEGUIDE BY WAY OF DIFFRACTION AT THE ED..(U) MISSISSIPPI UNIV UNIVERSITY DEPT OF ELECTRICAL ENGINEERING T H FARRIS ET AL. 1/1

UNCLASSIFIED MAR 85 N00014-81-K-0256 F/G 9/1 NL

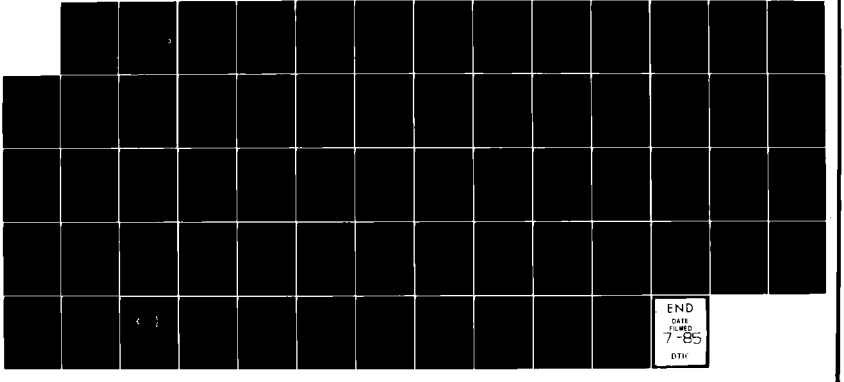

END
DATE FILMED
7-85
DTIC

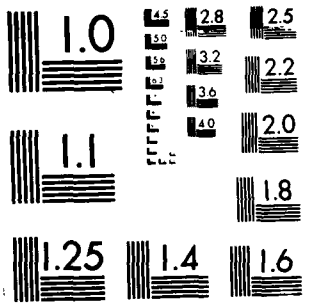

UNCLASSIFIED

SECURITY CLASSIFICATION OF THIS PAGE (When Data Entered)

REPORT DOCUMENTATION PAGE		READ INSTRUCTIONS BEFORE COMPLETING FORM
1. REPORT NUMBER N/A	2. GOVT ACCESSION NO.	3. RECIPIENT'S CATALOG NUMBER
4. TITLE (and Subtitle) Guided-mode Launching in a Slab Waveguide by way of Diffraction at the Edge of a Conducting Screen Residing on One Surface of the Slab		5. TYPE OF REPORT & PERIOD COVERED Final Technical Report 1 Jan 1983 - 1 Jan 1985 6. PERFORMING ORG. REPORT NUMBER N/A
7. AUTHOR(s) Timothy H. Farris and L. Wilson Pearson		8. CONTRACT OR GRANT NUMBER(s) N00014-81-K-0256
9. PERFORMING ORGANIZATION NAME AND ADDRESS Department of Electrical Engineering University of Mississippi University, MS 38677		10. PROGRAM ELEMENT, PROJECT, TASK AREA & WORK UNIT NUMBERS N/A
11. CONTROLLING OFFICE NAME AND ADDRESS ONR Resident Representative Georgia Institute of Technology Atlanta, GA 30332		12. REPORT DATE March 1985 13. NUMBER OF PAGES 59
14. MONITORING AGENCY NAME & ADDRESS(if different from Controlling Office) ONR Western Regional Office 1030 East Green Street Pasadena, CA 91106		15. SECURITY CLASS. (of this report) UNCALSSIFIED 15a. DECLASSIFICATION/DOWNGRADING SCHEDULE N/A

16. DISTRIBUTION STATEMENT (of this Report)

Distribution Unlimited

DISTRIBUTION STATEMENT A
Approved for public release
Distribution Unlimited

DTIC ELECTE JUN 10 1985 S D B

17. DISTRIBUTION STATEMENT (of the abstract entered in Block 20, if different from Report)

Distribution Unlimited

DISTRIBUTION STATEMENT A
Approved for public release
Distribution Unlimited

18. SUPPLEMENTARY NOTES

19. KEY WORDS (Continue on reverse side if necessary and identify by block number)

Diffraction, Scattering, Dielectric Interface, Slab Waveguide, Lateral Wave, Mode Launching

20. ABSTRACT (Continue on reverse side if necessary and identify by block number)

The behavior of electromagnetic fields in the presence of a dielectric waveguide or in the presence of a perfectly electrically conducting (p.e.c.) half plane constitute two general classes of problems in the study of electromagnetics. In this report we consider the case of a p.e.c. half plane residing on one surface of a dielectric slab waveguide in a homogeneous, lossless medium. A transverse magnetic plane wave impinges on the waveguide from the

Cont. on back

DD FORM 1 JAN 73 1473 EDITION OF 1 NOV 65 IS OBSOLETE
S/N 0102-014-6601

UNCLASSIFIED
SECURITY CLASSIFICATION OF THIS PAGE (When Data Entered)

side of the slab on which the half plane resides.

The boundary conditions for the electric field tangential to the half plane are cast in a form amenable to a Wiener-Hopf solution, from which the scattered electric field in the interior of the slab waveguide is obtained in terms of a radiation integral. This integral is evaluated using the method of steepest descents, and the resulting electric field is separated into a geometrical optics contribution, a contribution from diffraction at the edge of the half plane, a contribution from refraction by the waveguide, and guided-mode contributions.

The guided-mode contributions are expressed in terms of a launching coefficient, a transverse modal function, and a propagation factor. Some of the characteristics of each of these factors are investigated in the hope of gaining some insight into the physical phenomena of the problem. Among the conclusions is that the edge diffraction effect by the p.e.c. half plane plays a dominant role in the excitation of these modes.

TABLE OF CONTENTS

LIST OF FIGURES

CHAPTER I: INTRODUCTION

In this study we investigate the coupling of electromagnetic energy into a dielectric slab waveguide on one interface of which a perfectly electrically conducting (p.e.c.) half plane resides. The geometry is shown in Figure 1.1. The top face of the slab lies in the $y' = 0$ plane, with the p.e.c. screen residing on this face in the region $x' > 0$. The slab has a thickness t' and constituitive parameters (μ_0', ε_2'), where ε_2' may be complex. It is imbedded in a lossless medium with parameters (μ_0', ε_1'); both media are homogeneous and isotropic. A plane wave polarized transverse magnetic (TM) to the z' direction impinges on the top face of the slab at an angle θ $(0 < \theta < \pi)$. We assume there is no variation in the z' direction, so the problem is strictly two-dimensional.

The motivation for studying this problem is two-fold. First, this study is a continuation and extension of the work of Coblin (1983). Second, the geometry considered provides a canonical problem which can be useful in modeling metal-dielectric junctions. With a solution to this problem one is able to consider more complicated structures embodying, for example, discontinuities in the slab.

This investigation builds on the contributions of several authors. Heitman and van den Berg (1975) have studied the half plane in multi-

layered media, while Coblin (1983) has solved the problem of exterior scattering from a single, lossless slab screened by a half plane. Tamir and Felsen (1965a) have developed the asymptotic analysis of a line source in a slab. In addition, many authors have studied the propagation of electromagnetic fields in dielectric waveguides (e.g., Harrington (1961), Hessel (1969a)).

To solve this problem, one formulates an integral equation for the current on the p.e.c. screen by enforcing the condition that the total tangential electric field be zero on the p.e.c. screen. This integral equation is amenable to the Wiener-Hopf technique, which provides a solution for the Fourier transformation of the current on the screen. Multiplying this current by the transformed Green's function and then taking the inverse Fourier transformation gives an expression for the scattered electric field in the form of a spectral integral. The solution was carried to this stage by Coblin (1983), and his analysis is repeated here in order to establish consistent notation and to provide completeness.

Coblin carried out an asymptotic analysis for the fields in the two half spaces exterior to the slab but not for the fields in the slab itself. The purpose of this work is to complete the asymptotic analysis and provide an asymptotic representation for the fields within the slab.

A detailed description of the electric field within the slab is developed, and an effort is made to determine how various factors influence this field. To this end the representation is developed in

terms of contributions from the field that would be present in the absence of the p.e.c. screen, a collective lateral wave (steepest descent) field, a geometrical optics field, and a guided wave field. The guided wave field is represented by a modal expansion, from which a launching coefficient formulation is developed.

CHAPTER II: MATHEMATICAL DEVELOPMENT

2.1 Preliminary Developments

2.1.1 Definitions and Conventions

In this chapter we develop the solution to the electric field in the slab. Before beginning this development we must first state the conventions and definitions which are germane to the solution procedure; every attempt is made to remain consistent with the notation of Coblin (1983). The anaylsis is conducted for time-harmonic fields; a time convention of $e^{j\omega t}$ is assumed and suppressed throughout. With this convention Maxwell's equations have the form

$$\vec{\nabla} \cdot \vec{e} = \frac{\rho}{\epsilon'} \tag{2.1}$$

$$\vec{\nabla} \times \vec{e} = -\vec{m} - j\omega\mu'\vec{h} \tag{2.2}$$

$$\vec{\nabla} \cdot \vec{h} = 0 \tag{2.3}$$

$$\vec{\nabla} \times \vec{h} = \vec{j} + j\omega\epsilon'\vec{e} \tag{2.4}$$

where $\bar{e}$ and $\bar{h}$ are the electric and magnetic field intensities, respectively, ρ is the electric charge density, $\bar{j}$ is the electric

current density, $\bar{m}$ is the magnetic current density, and μ' and ε' are the constituitive parameters of the medium.

The media are passive, homogeneous, isotropic, and nonmagnetic, but the slab may be lossy. Each medium can be characterized by a wavenumber k', where

$$k' = \omega\sqrt{\mu'\varepsilon'} = k'_r - jk'_i$$

and

$$k'_r > 0 \ , \quad k'_i \geq 0 \ .$$

The analysis is carried out in the Fourier transformation, or spectral, domain, and throughout the chapter terms given in lowercase letters denote spatial domain quantities while uppercase letters denote spectral domain quantities. We define the Fourier transformation pair

$$A(k_x) = \mathcal{F}\{a(x)\} = \frac{1}{\sqrt{2\pi}} \int_{-\infty}^{\infty} a(x)\ e^{jk_x x}\ dx \tag{2.5}$$

$$a(x) = \mathcal{F}^{-1}\{A(k_x)\} = \frac{1}{\sqrt{2\pi}} \int_{-\infty+jc}^{\infty+jc} A(k_x)\ e^{-jk_x x}\ dk_x \tag{2.6}$$

where c is a real constant.

2.1.2 Normalization

For the sake of convenience we introduce a normalization in the spectral domain. Throughout the context, primed quantities (e.g., x') denote unnormalized quantities, and normalized quantities are unprimed (e.g., k_2). Defining the free space wavenumber $k_0 = \omega\sqrt{\mu_0\epsilon_0} = 2\pi/\lambda_0$,

$$k_j' = k_0 \cdot \sqrt{\mu_j \cdot \epsilon_j} , \quad \mu_j' = \mu_0\mu_j, \quad \epsilon_j' = \epsilon_0\epsilon_j, \quad j = 1,2.$$

Thus,

$$k_j' = k_0 \cdot k_j$$

where

$$k_j = \sqrt{\mu_j \cdot \epsilon_j} .$$

In order to be dimensionally consistent we must normalize the spatial variables to the free space wavenumber as follows:

$$\text{(normalized distance)} = k_0 \cdot \text{(unnormalized distance)},$$

so

$$x = k_0 \cdot x' ,$$

etc. For example, if the slab had a thickness of one half the free space wavelength, the normalized thickness would be

$$t = k_0 \cdot t' = \frac{2\pi}{\lambda_0} \cdot \frac{\lambda_0}{2} = \pi \ .$$

This normalization ensures that $k \cdot x = k' \cdot x'$, etc., and that the normalized quantities are dimensionless.

2.2 Development of Integral Equation

2.2.1 Integral Equation for Current on Slab

Boundary conditions require that the total tangential electric field be zero along the p.e.c. half plane. For the TM case this means that the total z'-directed electric field component, $e_z(x',y')$, be zero for $y'=0$, $x'>0$. We partition $e_z(x',y')$ into the sum of two terms,

$$e_z(x',y') = e_z^{NP}(x',y') + e_z^{R}(x',y') \ , \tag{2.7}$$

where the following definitions have been made:

$$e_z^{NP}(x',y') = \left\{ \begin{array}{l} \text{the total field which would result} \\ \text{with no p.e.c. screen--including the} \\ \text{incident field and the field scat-} \\ \text{tered by the slab} \end{array} \right.$$

$$e_z^{R}(x',y') = \left\{ \begin{array}{l} \text{the field radiated by the current} \\ \text{on the p.e.c. screen} \end{array} \right.$$

After applying the normalization discussed in the previous section,

$$k_x = k_1 \sin\alpha \ , \qquad \alpha = u + jv, \tag{2.47}$$

$$dk_x = k_1 \cos\alpha \, d\alpha .$$

This α plane is periodic along the real axis with period 2π, so we are only interested in the interval $u \in (-\pi,\pi)$. The mapping has the effect of "unfolding" the branch cuts associated with $\pm k_1$ so that the bottom sheet of the spectral plane is exposed in the one-sheeted α plane. The integral may have singularities arising from $G(k_x,y)/G_+(k_x)$ on the now-exposed bottom sheet in the form of leaky wave poles in addition to the geometrical optics pole associated with $(k_x + k_1\cos\theta)$ and surface wave poles, also associated with $G(k_x,y)/G_+(k_x)$. Under the transformation (2.47) the integral in (2.46) may be written as

$$e_z^R(x,y) = \xi \int_\Gamma \frac{\cos\alpha \, G(k_1\sin\alpha, y) e^{-jk_1 x \sin\alpha}}{G_+(k_1\sin\alpha)(\sin\alpha + \cos\theta)} \, d\alpha \ . \tag{2.48}$$

where we have defined the coefficient ξ as

$$\xi = \frac{-jE_0\beta_1(k_1\cos\theta)G(k_1\cos\theta,0)}{2\pi G_-(-k_1\cos\theta)} \ . \tag{2.49}$$

The path Γ is shown in Figure 2.3 for the case of a lossless slab (k_2 real) to emphasize the location of Γ with respect to singularities in the α plane.

$$E_z^R(k_x,y) = \mu_0\sqrt{2\pi}\cdot J_+(k_x)G(k_x,y)$$

$$= \frac{-jE_0\beta_1(k_1\cos\theta)G(k_1\cos\theta,0)G(k_x,y)}{\sqrt{2\pi}G_-(k_1\cos\theta)G_+(k_x)(k_x + k_1\cos\theta)}. \qquad (2.45)$$

The radiated field is found by taking the inverse Fourier transformation of this expression, or

$$e_z^R(x,y) = \mathcal{F}^{-1}\{E_z^R(x,y)\} = \frac{1}{\sqrt{2\pi}}\int_{-\infty+jc}^{\infty+jc} E_z^R(k_x,y)e^{-jk_xx}dk_x$$

$$= \frac{-jE_0}{2\pi}\cdot\frac{\beta_1(k_1\cos\theta)G(k_1\cos\theta,0)}{G_-(-k_1\cos\theta)}\int_P \frac{G(k_x,y)e^{-jk_xx}}{G_+(k_x)(k_x + k_1\cos\theta)}dk_x \qquad (2.46)$$

where the path P is the collapsed strip of analyticity shown in Figure 2.2.

2.3 Asymptotic Evaluation of the Radiation Integral

2.3.1 Mapping into the Angular Spectral Plane

For the purpose of asymptotically evaluating the integral in equation (2.46) via the steepest descent method, we map the spectral plane into an angular spectral plane, the α plane, using the transformation

$$P(k_x) = J_+(k_x)G_+(k_x) - S_+(k_x) = S_-(k_x) - \frac{B_-(k_x)}{G_-(k_x)} \qquad (2.43)$$

for all k_x.

Applying the edge condition at the edge of the p.e.c. screen and then investigating the asymptotic behavior of the functions in (2.43) shows that $P(k_x) \to 0$ as $|k_x| \to \infty$. Therefore, by Liouville's Lemma (Hille, 1959a),

$$P(k_x) = 0 \qquad \text{for all } k_x.$$

This allows us to solve for $J_+(k_x)$:

$$J_+(k_x) = \frac{S_+(k_x)}{G_+(k_x)}$$

$$= \frac{-jE_0\beta_1(k_1\cos\theta)G(k_1\cos\theta,0)}{\mu_0 2\pi G_-(-k_1\cos\theta)G_+(k_x)(k_x + k_1\cos\theta)} \quad . \qquad (2.44)$$

2.2.5 Radiation Integral

Having found expressions for the Fourier transformations of the current on the screen and the Green's function, we can find the transformation of the radiated field, $E_z^R(k_x,y)$, which is given by

$$\frac{A_+(k_x)}{G_-(k_x)} = S_+(k_x) + S_-(k_x). \tag{2.39}$$

The decomposition of Coblin (1983) is valid for complex k_2, and can be accomplished by inspection. The functions $S_+(k_x)$ and $S_-(k_x)$ are given by

$$S_-(k_x) = \frac{A_+(k_x)}{G_-(k_x)} - \frac{A_+(k_x)}{G_-(-k_1\cos\theta)}, \tag{2.40}$$

$$S_+(k_x) = \frac{A_+(k_x)}{G_-(-k_1\cos\theta)}. \tag{2.41}$$

With the decomposition in hand, we can rewrite the Wiener-Hopf equation as

$$J_+(k_x)G_+(k_x) - S_+(k_x) = S_-(k_x) - \frac{B_-(k_x)}{G_-(k_x)}, \quad \tau_- < \tau < \tau_+. \tag{2.42}$$

Note that the left hand side is composed of functions analytic for $\tau > \tau_-$ and the right hand side is composed of functions analytic for $\tau < \tau_+$. Therefore, we can analytically continue (2.42) into the entire spectral plane where each side of (2.42) is equal to an entire function $P(k_x)$:

$$G_+(k_x) = \begin{cases} \left(\frac{-2\sqrt{2\pi}}{\omega}\right)^{1/2} \frac{\beta_1}{\sqrt{k_1 - k_x}} G(k_x,0) e^{H(k_x)}, & \mathrm{Re}(k_x)>0 \\ \left(\frac{-\omega}{2\sqrt{2\pi}}\right)^{1/2} \frac{e^{H(k_x)}}{\sqrt{k_1 - k_x}}, & \mathrm{Re}(k_x)<0 \end{cases} \tag{2.34}$$

$$G_-(k_x) = G_+(-k_x), \tag{2.35}$$

where

$$H(k_x) = \frac{k_x}{2} \int_0^1 \frac{\mathrm{Ln}\{F[\delta(\zeta)]\}}{\cos^2\left(\frac{\pi\zeta}{2}\right) + k_x^2 \sin^2\left(\frac{\pi\zeta}{2}\right)} \, d\zeta \tag{2.36}$$

and

$$\delta(\zeta) = j\cot\left(\frac{\pi\zeta}{2}\right). \tag{2.37}$$

The validity of the factorization has been checked numerically for $\varepsilon_2' = (4 - j1)\varepsilon_0$. The r.m.s. error in $(G - G_+G_-)/G$ was observed to be less than 10^{-5} over both the top and bottom sheets of the k_x plane.

This factorization allows us to rewrite the Wiener-Hopf equation as

$$J_+(k_x)G_+(k_x) = \frac{A_+(k_x)}{G_-(k_x)} - \frac{B_-(k_x)}{G_-(k_x)}, \qquad \tau_- < \tau < \tau_+. \tag{2.38}$$

We must now decompose the quotient A_+/G_- into two functions $S_+(k_x)$ and $S_-(k_x)$ such that $S_+(k_x)$ is analytic for $\tau > \tau_-$, $S_-(k_x)$ is analytic for $\tau < \tau_+$, and

$$F(k_x) = 2\beta_1 \frac{(\beta_1 - \beta_2)e^{-j\beta_2 t} - (\beta_1 + \beta_2)e^{+j\beta_2 t}}{(\beta_1 - \beta_2)^2 e^{-j\beta_2 t} - (\beta_1 + \beta_2)^2 e^{+j\beta_2 t}} \tag{2.32}$$

The first term of $G(k_x,0)$ factors by inspection into

$$\frac{-\omega}{2\sqrt{2\pi}\beta_1} = \left(\left(\frac{-\omega}{2\sqrt{2\pi}} \right)^{1/2} \cdot \frac{1}{\sqrt{k_1 - k_x}} \right) \times \left(\left(\frac{-\omega}{2\sqrt{2\pi}} \right)^{1/2} \cdot \frac{1}{\sqrt{k_1 + k_x}} \right). \tag{2.33}$$

As $|k_x| \to \infty$, $\beta_1 \to \sqrt{k_x^2}$ and $\beta_2 \to \sqrt{k_x^2}$ for any k_2, real or complex. Since, on the top sheet of the spectral plane, $\mathrm{Im}(\beta_2) < 0$, $\mathrm{Re}(j\beta_2 t) \to \infty$ as $|k_x| \to \infty$. Therefore,

$$F(k_x) \sim 2\beta_1 \frac{0 - (\beta_1 + \beta_2)e^{+j\beta_2 t}}{0 - (\beta_1 + \beta_2)^2 e^{+j\beta_2 t}}$$

$$\sim 1.$$

These arguments, put forth by Coblin (1983), are restricted to lossless media and are made for k_x on the top sheet only; they are unaffected if the slab material is lossy. The leaky wave poles for the slab lie in quadrants two and four of the bottom sheet, just as the proper surface wave poles lie in quadrants two and four of the top sheet. Therefore, the factorization is valid on the bottom sheet, also, and it is given by

$$b_-(x) \propto Ce^{jk_1 x}.$$

Considering an infinitesimal amount of loss in the exterior medium, $b_-(x)$ must go to zero as $x \to -\infty$. Using this knowledge we determine that $B_-(k_x)$ is analytic for $\tau < \mathrm{Im}(-k_1)$. (See Figure 2.1.)

Since we have already shown that $G(k_x,0)$ is analytic and nonzero in the strip $\mathrm{Im}(k_1) < \tau < \mathrm{Im}(-k_1)$, the Wiener-Hopf equation (2.30) exists in the strip $\mathrm{Im}(-k_1\cos\theta) < \tau < \mathrm{Im}(-k_1)$. When the infinitesimal loss in the exterior medium goes to zero, this strip collapses to the real axis as shown in Figure 2.2.

The next step in the Wiener-Hopf solution is to factor $G(k_x,0)$ into two functions $G_+(k_x)$ and $G_-(k_x)$ such that $G_+(k_x)$ is analytic and nonzero for $\tau > \tau_-$, $G_-(k_x)$ is analytic and nonzero for $\tau < \tau_+$, and

$$G(k_x,0) = G_+(k_x)G_-(k_x).$$

Coblin (1983) has found this factorization for a lossless slab. In order for this factorization to be valid for a lossy slab, $G(k_x,0)$ must be free of zeros and singularities in the strip of analyticity, $\tau_- < \tau < \tau_+$ (which, as we have shown, it is), and we must be able to separate it into a product of two terms, one of which must limit to the value 1 as $|k_x| \to \infty$ in the strip. We can write $G(k_x,0)$ as

$$G(k_x,0) = \frac{-\omega}{2\sqrt{2\pi\beta_1}} \cdot F(k_x), \tag{2.31}$$

where

This allows us to rewrite (2.12) as

$$a_+(x) - b_-(x) = \frac{1}{\sqrt{2\pi}} \int_{-\infty}^{\infty} j_+(x_0) g(x_0,x;0)dx_0,$$

$$-\infty < x < \infty. \qquad (2.29)$$

The right hand side of equation (2.29) is simply the convolution of j_+ and g, so after applying the Fourier transformation to both sides of the equation we obtain the Wiener-Hopf equation

$$A_+(k_x) - B_-(k_x) = J_+(k_x)G(k_x,0), \quad \tau_- < \tau < \tau_+. \qquad (2.30)$$

For this transformation to be valid the functions A_+, B_-, J_+, and G must be analytic in the strip $\tau_- < \tau < \tau_+$, and G must be nonzero in the same strip. We have already shown that A_+ is analytic for $\tau > \mathrm{Im}(-k_1\cos\theta)$. The current $j(x,0)$ must have the same asymptotic behavior as $x \to \infty$ as the scattered field, and thus it must have the same asymptotic behavior as the incident field in order to satisfy boundary conditions everywhere along the screen. Thus $j(x,0)$ has the same asymptotic behavior as $x \to \infty$ as $a_+(x)$, and $J_+(k_x)$ must be analytic in the same region in which $A_+(k_x)$ is analytic, namely, $\tau > \mathrm{Im}(-k_1\cos\theta)$.

We next note that $b_-(x)$ is proportional to the scattered field on the top face of the slab (y=0) for $x < 0$. Along the slab, as $x \to -\infty$ we expect this field to show the same behavior as a negative-traveling plane wave, or

(Coblin, 1983). This will be discussed after we evaluate the field integral.

Considering a lossy slab and introducing an infinitesimal amount of loss in the exterior medium, we see that either

$$\mathrm{Im}(-k_1) \leq \mathrm{Im}(\text{poles, zeros}) \leq \mathrm{Im}(-k_2)$$

or

$$\mathrm{Im}(k_2) \leq \mathrm{Im}(\text{poles, zeros}) \leq \mathrm{Im}(k_1).$$

Thus, $G(k_x,y)$ is analytic and nonzero for

$$\mathrm{Im}(k_1) \leq \tau \leq \mathrm{Im}(-k_1).$$

2.2.4 Wiener-Hopf Solution for $J_z(k_x)$

In the Wiener-Hopf procedure (c. f. Mittra and Lee, 1971a), we seek the Fourier transformation of equation (2.12). In order to accomplish this transformation, we must extend the limits of the integral in (2.12) to include all x (i.e., $x \in (-\infty,\infty)$). Therefore, we are forced to introduce the functions $b_-(x)$ and $j_+(x)$ defined by

$$b_-(x) = \begin{cases} 0, & x > 0 \\ \text{unknown function}, & x < 0 \end{cases} \tag{2.27}$$

$$j_+(x) = \begin{cases} j_z(x), & x > 0 \\ 0, & x < 0 \end{cases} \tag{2.28}$$

$$A_z(k_x,y) = \begin{cases} T_u e^{-j\beta_1 y}, & y \geq 0 \\ \dfrac{\gamma_u(k_x,0)\gamma_d(k_x,y)}{\sqrt{2\pi}\,W}, & -t \leq y \leq 0 \\ T_d e^{j\beta_1 y}, & y \leq -t \end{cases} \tag{2.22}$$

where

$$\gamma_u(k_x,y) = e^{-j\beta_2 y} + \Gamma_u e^{+j\beta_2 y}, \tag{2.23}$$

$$\gamma_d(k_x,y) = e^{+j\beta_2 y} + \Gamma_d e^{-j\beta_2 y}, \tag{2.24}$$

$$W = \gamma_d \frac{\partial \gamma_u}{\partial y} - \gamma_u \frac{\partial \gamma_d}{\partial y} = -j2\beta_2(1 - \Gamma_u\Gamma_d), \tag{2.25}$$

and T_u, T_d, Γ_u, and Γ_d can be found by applying the boundary conditions. When this is done, we find

$$G(k_x,y) = -j\omega A_z(k_x,y)$$

$$= \frac{-\omega}{\sqrt{2\pi}} \cdot \frac{(\beta_1 - \beta_2)e^{-j\beta_2(y+t)} - (\beta_1 + \beta_2)e^{+j\beta_2(y+t)}}{(\beta_1 - \beta_2)^2 e^{-j\beta_2 t} - (\beta_1 + \beta_2)^2 e^{+j\beta_2 t}} \tag{2.26}$$

in the slab.

The poles and zeros of $G(k_x,y)$ on the top sheet of the spectral plane lie between k_1, k_2 and $-k_1$, $-k_2$ (Hessel, 1969b). The poles correspond to surface waves for a dielectric slab, and, for $y = 0$, the zeros correspond to surface waves for a grounded dielectric slab

$$\vec{a}(x,y) = \hat{z}\, a_z(x,y) \tag{2.16}$$

such that

$$e_z(x,y) = -j\omega a_z(x,y) \tag{2.17}$$

$$\vec{h}(x,y) = \frac{1}{\mu_0} \vec{\nabla} \times [\hat{z} a_z(x,y)]. \tag{2.18}$$

The potential $a_z(x,y)$ is a solution to the equation

$$\left\{ \vec{\nabla}^2_{xy} + k_i^2 \right\} a_z(x,y) = \begin{cases} -\delta(x)\delta(y), & i = 2 \\ 0, & i = 1 \end{cases} \tag{2.19}$$

subject to the boundary conditions which require that a_z and its derivatives be continuous at $y = 0$ and $y = -t$. Application of the Fourier transformation to this equation yields

$$\left\{ \frac{\partial^2}{\delta y^2} + (k_i^2 - k_x^2) \right\} A_z(k_x,y) = \begin{cases} -\frac{1}{\sqrt{2\pi}} \delta(y), & i = 2 \\ 0, & i = 1 \end{cases} \tag{2.20}$$

and the transformed Green's function is given by

$$G(k_x,y) = -j\omega A_z(k_x,y). \tag{2.21}$$

Using the approach outlined by Felsen and Marcuvitz (1973a), we obtain

also in the region in the k_x plane in which this transformation is analytic. The transformation of $a_+(x)$ is given by

$$A_+(k_x) = \mathcal{F}\{a_+(x)\} = \frac{1}{\mu_0 2\pi} \int_0^\infty e_z^{NP}(x,0)\, e^{jk_x x}\, dx$$

$$= \frac{j2E_0\beta_1(k_1\cos\theta)G(k_1\cos\theta,0)}{\mu_0\omega\sqrt{2\pi}\,(k_x + k_1\cos\theta)} \times$$

$$\left\{ 1 - \lim_{b\to\infty} e^{j(k_x + k_1\cos\theta)b} \right\} \qquad (2.14)$$

The limit in (2.14) exists and is 0 only when

$$\tau > \mathrm{Im}(-k_1\cos\theta) = \tau_-, \qquad k_x = \sigma + j\tau.$$

Thus, the analytic function $A_+(k_x)$ is given by

$$A_+(k_x) = \frac{j2E_0\beta_1(k_x\cos\theta)G(k_x\cos\theta,0)}{\mu_0\omega\sqrt{2\pi}\,(k_x + k_1\cos\theta)},$$

$$\tau > \mathrm{Im}(-k_1\cos\theta). \qquad (2.15)$$

2.2.3 Fourier Transformation of the Green's Function

In order to solve for the current on the half plane, we must find the Fourier transformation of the Green's function for a line source on the top face of the slab, $G(k_x,y)$, and find the region in the spectral plane where $G(k_x,y)$ is analytic and nonzero. To this end, we temporarily introduce the concept of a magnetic vector potential

$$e_z^R(x',y') = \mu_0 \int_0^\infty j_z(x_0) g(x',x_0;y')\, dx_0. \tag{2.11}$$

Application of the boundary conditions produces the integral equation

$$e_z^{NP}(x',0) = -\mu_0 \int_0^\infty j_z(x_0) g(x',x_0;0)\, dx_0, \qquad 0 < x' < \infty. \tag{2.12}$$

This equation is of a form suitable for application of the Wiener-Hopf technique, which, when applied, will give a solution for the Fourier transformation of the current on the half plane. To find this solution we must find the Fourier transformation of the no-plane field and of the Green's function.

2.2.2 Fourier transformation of $e_z^{NP}(x,y)$

To apply the Wiener-Hopf technique, we define the function

$$a_+(x) = \begin{cases} \frac{1}{\mu_0\sqrt{2\pi}}\, e_z^{NP}(x,0), & x > 0 \\ 0, & x < 0. \end{cases} \tag{2.13}$$

We are not only interested in the Fourier transformation of $a_+(x)$, but

the e_z^{NP}, or "no-plane," component of the field can be found by solving the problem of a plane wave of magnitude E_0, given by

$$e_z^{inc}(x,y) = E_0\, e^{jk_1(x\cos\theta + y\sin\theta)}\,, \tag{2.8}$$

incident upon a dielectric slab. The no-plane component, given by Coblin (1983), is

$$e_z^{NP}(x,0) = -\frac{2\sqrt{2\pi}}{\omega} E_0\beta_1(k_1\cos\theta)G(k_1\cos\theta,0)\, e^{jk_1x\cos\theta}, \tag{2.9}$$

where we have rearranged the expression to include $G(k_x,y)$, the Fourier transformation of the Green's function for a line source on the top face of the slab, and

$$\beta_i(k_x) = \sqrt{k_i^2 - k_x^2}\,, \qquad i = 1,2, \tag{2.10}$$

where we choose

$$\mathrm{Im}(\beta_1) < 0, \text{ or, if } \mathrm{Im}(\beta_1) = 0, \mathrm{Re}(\beta_1) > 0.$$

Choosing the sign of the square root in this manner ensures that the fields satisfy a radiation condition at infinity and defines the top sheet of the spectral plane.

We can determine e_z^R from the convolution of the current induced on the half plane and the Green's function for a z'-directed line source on the slab, i.e.,

2.3.2 Deformation of Γ to the Steepest Descent Path

To evaluate (2.48) using the steepest descent method, we must find the path along which the exponential in the integrand of (2.48) decays most rapidly--the steepest descent path, or SDP, which passes through the saddle point, α_s, where the derivative of the argument of the exponential with respect to α is zero; i.e.,

$$\frac{d}{d\alpha}(-jk_1 x \sin\alpha)\Big|_{\alpha_s} = 0.$$

The saddle points in the region of interest are $\alpha_s = \pi/2$ for $x > 0$ and $\alpha_s = -\pi/2$ for $x < 0$. The SDP lies on the contour through the saddle point characterized by the imaginary part of the argument of the exponential in (2.48) being constant. It is given by points that satisfy

$$\mathrm{Im}(-jk_1 x \sin\alpha) = \mathrm{Im}(-jk_1 x \sin\alpha_s) = -k_1|x| \ , \tag{2.50}$$

or

$$\sinh(v) = \cot(u) \tag{2.51}$$

where

$$u \in \begin{cases} (0,\pi), & x > 0,\ \alpha_s = \pi/2 \\ (-\pi,0), & x < 0,\ \alpha_s = -\pi/2. \end{cases}$$

Thus, we will be concerned with two steepest descent paths, SDP^+ through $\alpha_s = \pi/2$ and SDP^- through $\alpha_s = -\pi/2$. These paths are shown in Figure

2.4. When the path Γ is deformed to the SDP, singularities will be swept, thus contributing residue terms to $e_z^R(x,y)$ in addition to the contribution from the evaluation of the integral along the SDP. This shows that $e_z^R(x,y)$ is made up of components from four contributors:

1. The result from the evaluation of (2.48) along the SDP.
2. The residue obtained from the capture of the geometrical optics pole.
3. The residue obtained from the capture of any number of surface wave poles.
4. The residue obtained from the capture of any number of leaky wave poles.

Tamir and Felsen (1965b) have found that the contribution to $e_z^R(x,y)$ from the SDP integration, $e_z^{SDP}(x,y)$, is equivalent to a collective lateral wave as shown in Figure 2.5. The contribution from the geometrical optics pole, $e_z^{GO}(x,y)$, accounts for the shadowing of the incident field by the p.e.c. screen. The contributions from the surface and/or leaky wave poles, $e_z^M(x,y)$, can be characterized as a series of modes propagating and/or decaying in the slab in a manner similar to that in a dielectric waveguide. The total radiated field is found by summing all the individual contributors:

$$e_z^R(x,y) = e_z^{SDP}(x,y) + e_z^{GO}(x,y) + \Sigma\, e_z^M(x,y). \tag{2.52}$$

Each component of $e_z^R(x,y)$ is considered in the following.

2.3.3 SDP Integral

The contribution from $e_z^{SDP}(x,y)$ is given by the integral

$$e_z^{SDP}(x,y) = \xi \int_{SDP} \frac{\cos\alpha\, G(k_1 \sin\alpha, y) e^{-jk_1 x \sin\alpha}}{G_+(k_1 \sin\alpha)(\sin\alpha + \cos\theta)} \, d\alpha. \tag{2.53}$$

This integral can be solved in a straight-forward manner by the steepest descent method (Felsen and Marcuvitz, 1973b, Mittra and Lee, 1971b). We note that (2.53) is of the form

$$e_z^{SDP}(x,y) = \int_{SDP} K(\alpha,y) e^{xq(\alpha)} \, d\alpha \tag{2.54}$$

where

$$K(\alpha,y) = \xi \frac{\cos\alpha\, G(k_1 \sin\alpha, y)}{G_+(k_1 \sin\alpha)(\sin\alpha + \cos\theta)} \tag{2.55}$$

and

$$q(\alpha) = \pm jk_1 \sin\alpha \quad \text{for } x \lessgtr 0. \tag{2.56}$$

Making the substitution

$$s^2 = q(\alpha_s) - q(\alpha) \tag{2.57}$$

we note that $\mathrm{Im}\{q(\alpha)\}$ is constant along the SDP, so s is real along the SDP. This allows us to write (2.53) as

$$e_z^{SDP}(x,y) = e^{-j|k_1 x|} \int_{-\infty}^{\infty} M(s,y) e^{-xs^2}\, ds\ , \tag{2.58}$$

$$M(s,y) = K(\alpha,y) \left.\frac{d\alpha}{ds}\right|_{\alpha \text{ on SDP}}\ . \tag{2.59}$$

We can express this integral as an asymptotic series for large $|k_1 x|$:

$$e_z^{SDP}(x,y) \sim e^{-j|k_1 x|} \sum_{n=0}^{\infty} \left\{ \frac{M^{2n}(0,y)}{(2n)!} \left\{ \frac{-d^n}{(dk_1 x)^n} \left\{ \frac{\pi}{k_1 x} \right\}^{1/2} \right\} \right\},$$

$$\text{as } |k_1 x| \to \infty. \tag{2.60}$$

The first term of this series is zero due to the factor $\cos(\alpha)$, which is zero for $\alpha = \alpha_s$, so the second term is the dominant one, and

$$e_z^{SDP}(x,y) \sim \frac{j\xi k_1}{2\sqrt{\pi}\beta_{21}} \cdot \left\{ \frac{-2\sqrt{2\pi}}{\omega} \right\}^{1/2} \cdot Y(y) \cdot |k_1 x|^{-3/2} \cdot$$

$$e^{+j\left\{\frac{3\pi}{4} - |k_1 x|\right\}}, \qquad |k_1 x| \to \infty \tag{2.61}$$

where

$$Y(y) = \begin{cases} \dfrac{-e^{-H(k_1)}}{2\sqrt{k_1}(\cos\theta + 1)\cos^2(\beta_{21}t)} \cdot \sin(\beta_{21}y), & x > 0 \\ \dfrac{j4\sqrt{k_1}e^{H(k_1)}}{\beta_{21}(\cos\theta - 1)} \cdot \left\{ \dfrac{\tan[\beta_{21}(\frac{t}{2})]}{\cos[\beta_{21}(\frac{t}{2})]} \cdot \sin[\beta_{21}(y+\frac{t}{2})] + \right. & \\ \left. \dfrac{\cot[\beta_{21}(\frac{t}{2})]}{\sin[\beta_{21}(\frac{t}{2})]} \cdot \cos[\beta_{21}(y+\frac{t}{2})] \right\}, & x < 0, \end{cases} \tag{2.62}$$

and

$$\beta_{21} = \beta_2(k_1). \tag{2.63}$$

This expression represents a collective lateral wave made up of a finite summation of lateral waves as shown in Figure 2.5 (Tamir and Felsen 1965). Each lateral wave in the collection propagates for a unique distance in the exterior medium and undergoes a unique number of reflections into the dielectric slab at the critical angle. This critical angle is simply the angle of total internal reflection θ_c given by

$$\sin(\theta_c) = \sqrt{\epsilon_1/\epsilon_2}\ .$$

2.3.4 Uniform SDP Result

The contribution from $e_z^{SDP}(x,y)$ exhibits singular behavior for incidence angles near π for $x > 0$ and for incidence angles near 0 for $x < 0$. To correct for this behavior, the uniform SDP evaluation method (Felsen and Marcuvitz, 1973c) is applied and leads to a result that has no singular behavior at these angles. It is given by

$$\left\{e_z^{SDP}(x,y)\right\}_{unif} \sim \frac{\sqrt{2}\,\mathrm{sgn}(x)E_0}{\omega}\beta_1(k_1\cos\theta)G(k_1\cos\theta,y)\times$$

$$\left\{2Q\left\{\sqrt{|k_1x| + k_1x\cos\theta}\; e^{j\pi/4}\right\}e^{jk_1x\cos\theta} + \right.$$

$$\left.\frac{e^{-j|k_1x|}}{\sqrt{|k_1x| + k_1\cos\theta}}\left\{e^{-j\pi/4} - \frac{e^{j\pi/4}}{2(|k_1x| + k_1x\cos\theta)}\right\}\right\} -$$

$$\frac{2\pi\xi k_1}{\omega\beta_{21}}\cdot\left\{\frac{-\omega}{2\sqrt{2\pi}}\right\}^{1/2}\cdot Y(y)\cdot e^{-j\left\{\frac{3\pi}{4} + |k_1x|\right\}} \qquad (2.64)$$

where $Y(y)$ and β_{21} are given in (2.62) and (2.63), respectively, and

$$Q(y) = \int_y^\infty e^{-x^2}dx. \qquad (2.65)$$

2.3.5 Geometrical Optics Contribution

The geometrical optics field accounts for the shadowing effect of the screen. It arises from a singularity in the integrand of (2.46), the geometrical optics pole, at $k_x = -k_1\cos\theta$. In an asymptotic solution we would expect to encounter this field when $x > 0$ and not when $x < 0$. This is exactly what we find; as a consequence of the Wiener-Hopf solution procedure, the geometrical optics pole, $\alpha_{go} = \theta - \pi/2$, always lies below the path Γ and in the interval $[-\pi/2,\pi/2]$ on the real axis of the α plane. Thus, it is swept by the deformation to SDP^+ (i.e., observaton points under the half plane) and not by the deformation to SDP^-. This pole is encircled in the negative (clockwise) direction, therefore the geometrical optics contribution is given by

$$e_z^{GO}(x,y) = -j2\pi\xi U(x)\cdot \mathrm{Res}\left\{\frac{\cos\alpha G(k_1\sin\alpha,y)e^{-jk_1x\sin\alpha}}{G_+(k_1\sin\alpha)(\sin\alpha+\cos\theta)};\ \alpha_{go}\right\}$$

$$= U(x)\cdot\frac{2\sqrt{2\pi}}{\omega}E_0\beta_1(k_1\cos\theta)G(k_1\cos\theta,y)e^{jk_1x\cos\theta} \qquad (2.66)$$

where $U(x)$ is the unit step function,

$$U(x) = \begin{cases} 1, & x > 0 \\ 0, & x < 0. \end{cases} \qquad (2.67)$$

We note that

$$e_z^{GO}(x,y) = -e_z^{NP}(x,y)$$

for $x > 0$. This is as expected, and shows that the geometrical optics field does indeed account for the shadowing from the screen by canceling the no-plane field.

2.3.6 Modal Contributions

The remaining contributions to the radiated field arise from poles of G/G_+ in the integrand of (2.46). Both surface wave poles on the top sheet and leaky wave poles on the bottom sheet may be swept in the deformation from Γ to SDP^+ or SDP^-, each pole contributing a residue term to $e_z^R(x,y)$. Each of these residue terms can be expressed as a product of a launching coefficient--$L(\theta,\alpha_p)$, a transverse (y direction) modal function--$\Phi(y,\alpha_p)$, and a longitudinal (x direction) propagation factor--an exponential function of x and α_p, where α_p denotes the value of the pole in the α plane. With this representation we have an efficient form to study separately the modal structure of the field, the factors that influence the launching of a mode, and the propagation of a mode.

For each pole of G/G_+ swept in the deformation to the steepest descent path,

$$e_z^M(x,y) = \pm j2\pi\xi \cdot \mathrm{Res}\left\{\frac{\cos\alpha G(k_1\sin\alpha,y)e^{-jk_1 x\sin\alpha}}{G_+(k_1\sin\alpha)(\sin\alpha+\cos\theta)};\ \alpha_p\right\} \qquad (2.68)$$

$$\text{for } x \lessgtr 0.$$

The evaluation of the residue is tedious but straightforward and the resulting expression can be rearranged into the desired representation,

$$e_z^M(x,y) = E_0 L(\theta,\alpha_p)\Phi(y,\alpha_p)e^{-jk_x^p x} \qquad (2.69)$$

where $k_x^p = k_1\sin\alpha_p$. The modes that result can be segregated into readily interpretable classes. Under the half plane, i.e., $x' > 0$, the electric field must vanish at $y' = 0$, and all modes are governed by this condition. For $x' < 0$ the slab is an open structure, and a mode set manifesting both odd and even symmetry about the center of the slab ($y' = -t'/2$) arise. Specifically, for $x' > 0$

$$L(\theta,\alpha_p) = \frac{\beta_1(k_1\cos\theta)\cot(\alpha_p)\beta_{2p}^2 G(k_1\cos\theta,0)e^{-H(k_x^p)}}{G_-(-k_1\cos\theta)(k_1\cos\theta+k_x^p)\sin(\beta_{2p}t)\sqrt{k_1+k_x^p}} \times \left\{\frac{-2\sqrt{2\pi}}{\omega}\right\}^{1/2} \times$$

$$\{[\beta_{1p}\cos(\beta_{2p}t) - \beta_{1p}\beta_{2p}t\sin(\beta_{2p}t)] +$$

$$j[\beta_{1p}^2 t\cos(\beta_{2p}t) + \beta_{2p}\sin(\beta_{2p}t)]\}^{-1}, \qquad (2.70)$$

$$\phi(y,\alpha_p) = \sin(\beta_{2p}y), \tag{2.71}$$

where

$$\beta_{1p} = \beta_1(k_1\sin\alpha_p), \tag{2.72}$$

$$\beta_{2p} = \beta_2(k_1\sin\alpha_p). \tag{2.73}$$

For $x' < 0$ odd modes are given by

$$L(\theta,\alpha_p) = \frac{\beta_1(k_1\cos\theta)\cot(\alpha_p)\beta_{2p}^2\sqrt{k_1 - k_x^p}G(k_1\cos\theta,0)e^{-H(k_x^p)}}{G_-(-k_1\cos\theta)(k_1\cos\theta + k_x^p)\sin[\beta_{2p}(\frac{t}{2})]}\times\left\{\frac{-2\sqrt{2\pi}}{\omega}\right\}^{1/2}\times\Lambda, \tag{2.74}$$

$$\Lambda = \{2[(\beta_{1p}^2 + \beta_{2p}^2)\cos(\beta_{2p}t) - \beta_{1p}^2\beta_{2p}t\sin(\beta_{2p}t)] + j[4\beta_{1p}\beta_{2p}\sin(\beta_{2p}t) + \beta_{1p}t(\beta_{1p}^2 + \beta_{2p}^2)\cos(\beta_{2p}t)]\}^{-1}, \tag{2.75}$$

$$\phi(y,\alpha_p) = \sin[\beta_{2p}(y+\tfrac{t}{2})] \tag{2.76}$$

with β_{1p} and β_{2p} given above, while the even modes are given by

$$L(\theta,\alpha_p) = \frac{\beta_1(k_1\cos\theta)\cot(\alpha_p)\beta_{2p}^2\sqrt{k_1 - k_x^p}G(k_1\cos\theta,0)e^{-H(k_x^p)}}{G_-(-k_1\cos\theta)(k_1\cos\theta + k_x^p)\cos[\beta_{2p}(\frac{t}{2})]}\times\left\{\frac{-2\sqrt{2\pi}}{\omega}\right\}^{1/2}\times\Lambda, \tag{2.77}$$

$$\phi(y,\alpha_p) = \cos[\beta_{2p}(y+\tfrac{t}{2})] \tag{2.78}$$

with β_{1p}, β_{2p}, and Λ given above.

The reader is reminded that these are large-x asymptotic field representations. The continuity of e_z at $x' = 0$ is embodied in the integral representation (2.48), which constitutes a complete expression for the field. The changing of asymptotic representations between $x' > 0$ and $x' < 0$ does not contradict continuity.

The remainder of this study will be devoted to an investigation of the poles of G/G_+ and the modal fields which arise from them.

CHAPTER III: ANALYSIS OF RESULTS

3.1 Preliminary Developments

In a uniform dielectric slab waveguide of thickness t and permittivity ϵ_2, electromagnetic energy can propagate as guided waves in the form of modes. These modes will propagate in the slab in the longitudinal direction and will radiate energy into the exterior medium in which the slab is imbedded. They can be separated into two types: modes that are odd with respect to the center of the slab and modes that are even with respect to the center of the slab. If the slab is grounded by placing a p.e.c. plane on one surface, image theory tells us that this must be equivalent to a dielectric slab waveguide of thickness 2t, but since each mode must individually satisfy boundary conditions along the ground plane, only those modes that are even with respect to the ground plane may exist (Figure 3.1). Both types of behavior should be evident in the problem under consideration. For large $|k_1 x|$ the portion of the slab under the p.e.c. half plane ($x > 0$) should behave as a grounded dielectric slab waveguide, and the portion of the slab not under the half plane ($x < 0$) should behave as a slab waveguide in uniform space. This behavior is apparent in the analysis of the poles that produce the guided wave terms and in the analysis of the modal expressions that result from these poles.

In addition to the geometrical optics pole, two types of poles are encountered in the evaluation of $e_z^R(x,y)$. Surface wave poles (SWP's) which lie on the top sheet of the spectral plane and leaky wave poles (LWP's) which lie on the bottom sheet may contribute field terms. The two types of poles give rise to two different types of waves (Hessel, 1969c). A surface wave, produced by a SWP, behaves as a propagating mode in a slab waveguide. It propagates in the longitudinal direction, attenuated only by losses in the slab. As it propagates, it radiates energy in the exterior medium. This radiation decays exponentially away from the slab, while the transverse variation is sinusoidal inside the slab (Figures 3.1 and 3.2.a). A LWP produces a leaky wave, which behaves much like an evanescent mode inside the slab in that it decays exponentially in the longitudinal direction. Therefore, it does not make a significant contribution to the total field in an asymptotic solution. However, since a LWP occurs on the bottom sheet of the spectral plane, a leaky wave will not satisfy a radiation condition in the transverse direction; it grows exponentially away from the slab (Figure 3.2.b). The leaky wave field will satisfy a radiation condition, though, because it only exists in a restricted portion of the spatial plane (Figure 3.2.c). In Figure 3.2.c the center line of the slab and the direction of growth of the leaky wave define an angle θ_{growth}, but the leaky wave pole only contributes a field term inside the wedge defined by the center line and the angle $\theta_{contr.}$. The angle θ_{growth} is always greater than $\theta_{contr.}$, ensuring that the leaky wave

field does satisfy a radiation condition in the region in which it exists.

3.2 Poles of G/G_+

The SWP's and LWP's are poles of the quotient $G(k_x,0)/G_+(k_x)$. Due to the factorization of $G(k_x,y)$ in the Wiener-Hopf procedure, this quotient takes two forms, one for $x > 0$ and one for $x < 0$. For $x > 0$, $\alpha_s = \pi/2$ and $\mathrm{Re}(k_1 \sin\alpha) > 0$, so

$$\frac{G(k_x,y)}{G_+(k_x)} = \left\{\frac{-\omega e^{-H(k_x)}}{2\sqrt{2\pi}\sqrt{k_1 + k_x}}\right\} \cdot \left\{\frac{-2\sqrt{2\pi}}{\omega}\right\}^{1/2} \cdot \left\{\frac{(\beta_1 - \beta_2)e^{-j\beta_2(y+t)} - (\beta_1 + \beta_2)e^{+j\beta_2(y+t)}}{(\beta_1 - \beta_2)e^{-j\beta_2 t} - (\beta_1 + \beta_2)e^{+j\beta_2 t}}\right\}, \tag{3.1}$$

while for $x < 0$, $\alpha_s = -\pi/2$ and $\mathrm{Re}(k_1 \sin\alpha) < 0$, so

$$\frac{G(k_x,y)}{G_+(k_x)} = \left\{\frac{-\omega e^{-H(k_x)}\sqrt{k_1 - k_x}}{\sqrt{2\pi}}\right\} \cdot \left\{\frac{-2\sqrt{2\pi}}{\omega}\right\}^{1/2} \cdot \left\{\frac{(\beta_1 - \beta_2)e^{-j\beta_2(y+t)} - (\beta_1 + \beta_2)e^{+j\beta_2(y+t)}}{(\beta_1 - \beta_2)^2 e^{-j\beta_2 t} - (\beta_1 + \beta_2)^2 e^{+j\beta_2 t}}\right\}. \tag{3.2}$$

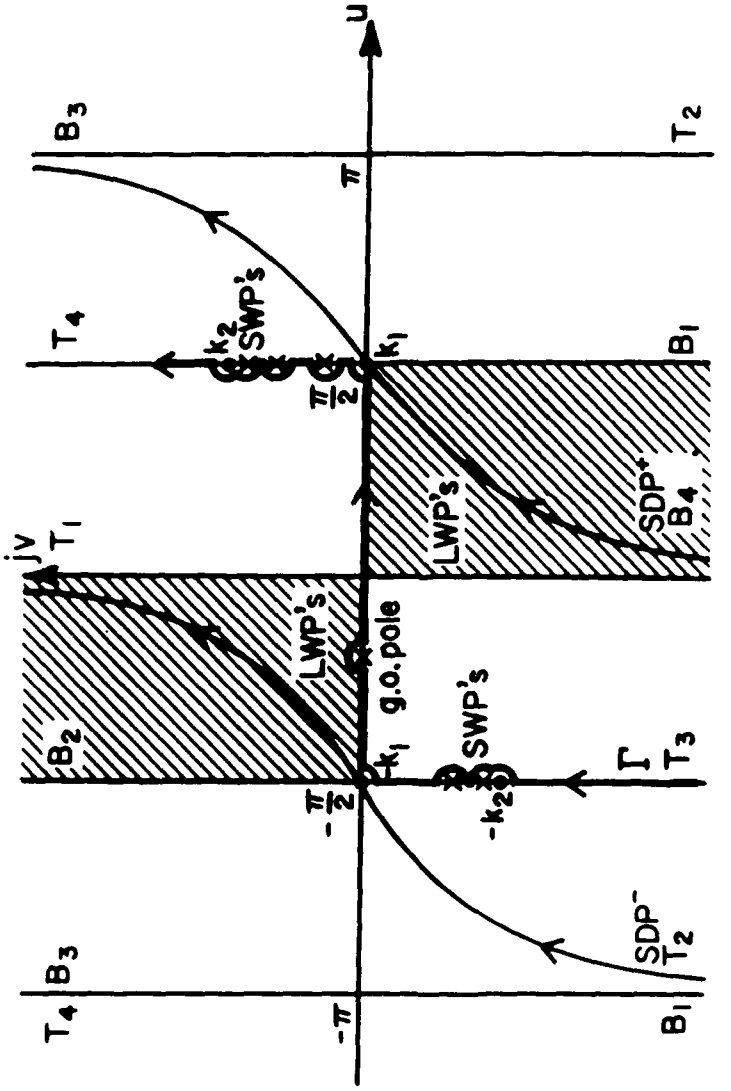

Figure 2.4. Deformation of Γ to the SDP.

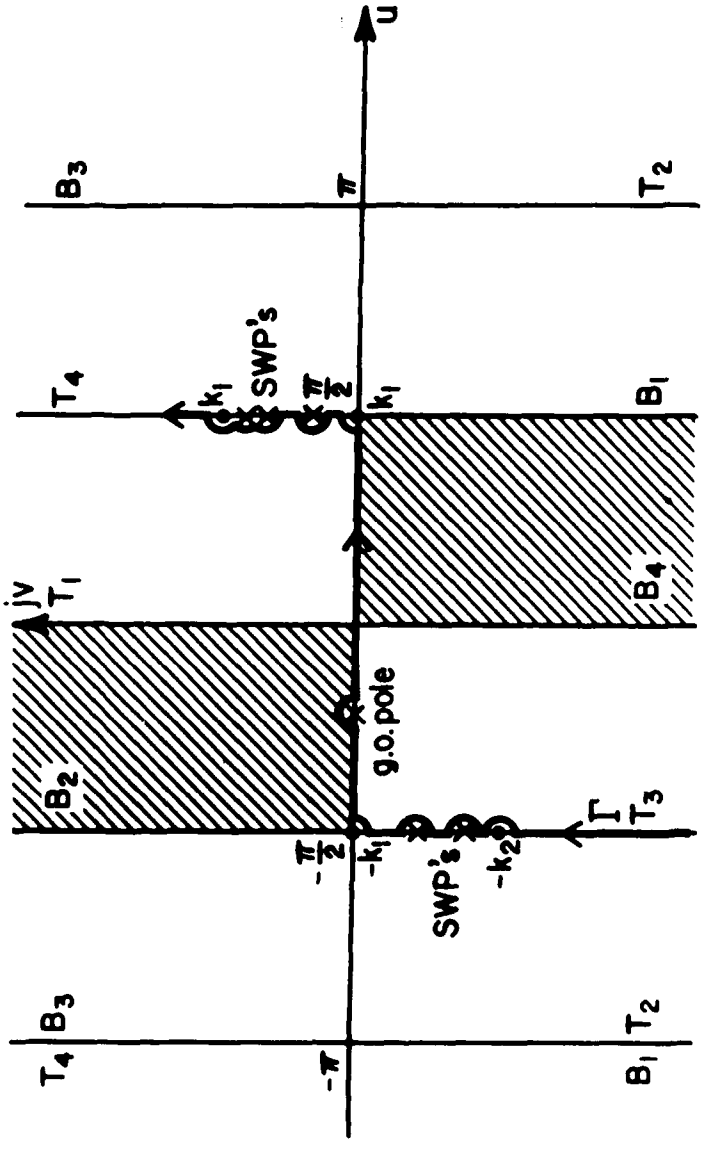

Figure 2.3. Mapping into the angular spectral plane for a lossless slab. Leaky wave poles map into the shaded region.

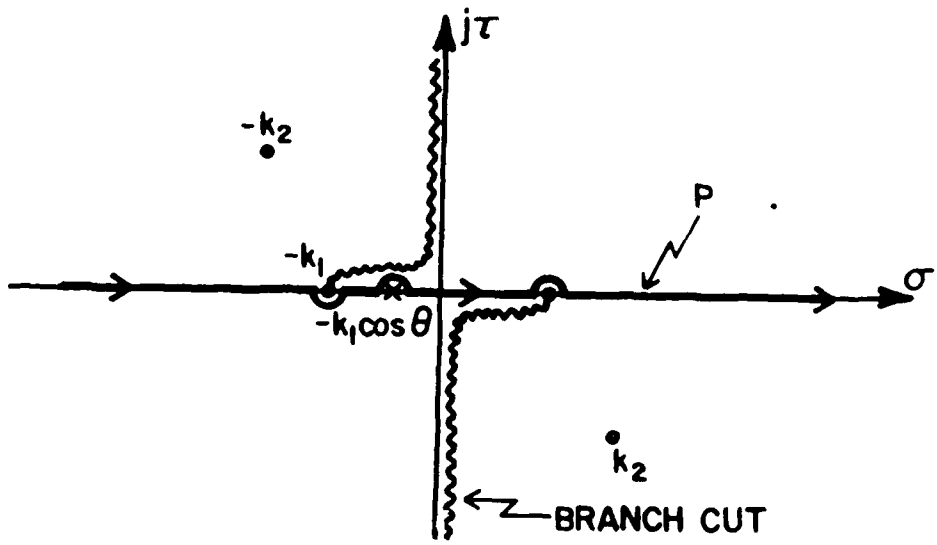

Figure 2.2. Integration path for the radiation integral showing the collapsed strip of analvticity.

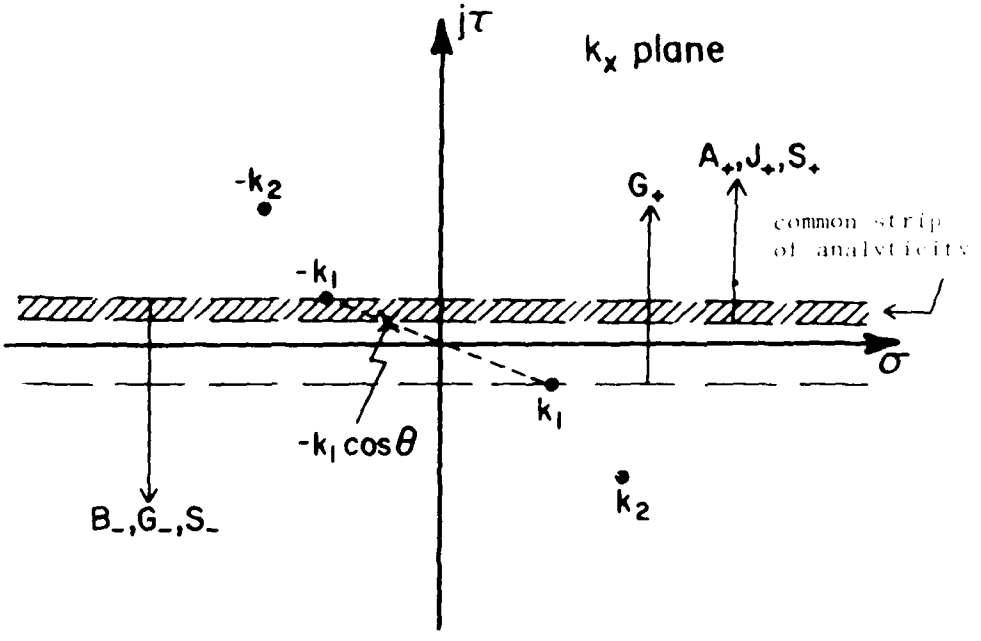

Figure 2.1. Regions of analyticity for the functions in the Wiener Hopf solution.

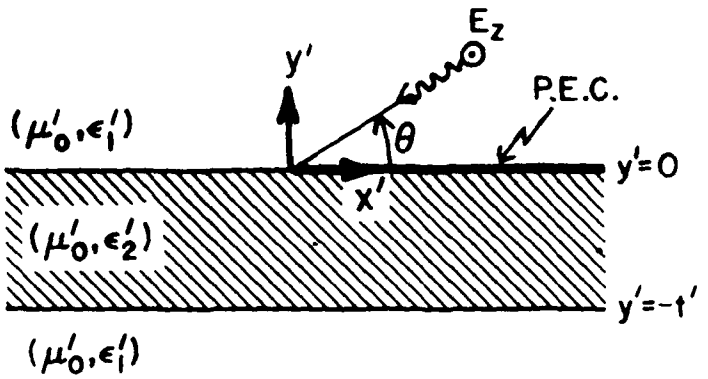

Figure 1.1. Geometry of the slab problem.

The physical properties of the slab and the location of the guided wave poles also had an effect on the launching of the modes. The large magnitudes of the launching coefficients was unexpected, and at present an adequate explanation is not available. Further study of this phenomenon is warranted.

With this solution completed for the geometry considered in this study, one is prepared to extend the work to more complicated slab structures or to delve deeper into the physical mechanisms at work in the scattering process.

CHAPTER IV: CONCLUSION

In this study we have investigated the scattering of an electromagnetic plane wave by a dielectric slab shielded by a p.e.c. half plane residing on the top face of the slab. We developed solutions for the Green's function for a line source on the slab and for the current on the half plane, extending the results to accomodate losses in the slab. The total field was expressed as the sum of a no-plane field, which accounted for the effects of the slab and the incident plane wave, and a radiated field which accounted for the effect of the screen. This radiated field was developed asymptotically as the sum of a collective lateral wave contribution, a geometrical optics contribution, and contributions from guided wave poles. The contributions from the guided wave poles were expressed as modes giving rise to surface waves or leaky waves. We were able to state these modes as the product of a transverse modal function, a propagation factor, and a launching coefficient. This launching coefficient played a similar role in the launching of these guided waves to that of a diffraction coefficient in diffraction theory. The launching of the guided modes was investigated in some detail, and an effort was made to explain the physical mechanisms that affected the launching of these guided modes. It was observed that the edge diffraction effect played a major role in the mode-launching phenomenon.

Another interesting effect is seen in the launching coefficients for a slab in free space with permittivity $10\epsilon_0$ and thickness $\lambda_0/2$ (Figure 3.8). For this case the launching coefficient is not zero for $\theta = 0$ and $\theta = \pi$. Normally $\beta_1(k_1 \cos\theta)$, which is zero for $\theta = 0$ and $\theta = \pi$, forces the entire launching coefficient to zero at these angles. For these parameters, however, there is a pole of $G(\pm k_1, 0)$ that cancels the zero of $\beta_1(\pm k_1)$. This phenomenon will occur whenever

$$t\sqrt{\epsilon_2 - \epsilon_1} = n\pi, \quad n \text{ an integer.}$$

When this relationship is satisfied, the electrical thickness of the slab is such that the no-plane field is no longer zero for $\theta = 0$ or $\theta = \pi$, and modes can be excited.

shapes are relatively independent of the location of the poles that produce them. This further supports the hypothesis that edge diffraction dominates the launching of modes and also shows that the properties of the slab influence the shape of $L(\theta,\alpha_p)$ more than the location of the poles.

The launching coefficients have only one or two local maxima over the range of θ. The number of maxima remains the same for each pole found for a given set of parameters. For slabs that are electrically thin (e.g., $\varepsilon_2' = 4\varepsilon_0$, $t' = 0.2\lambda_0$, $\varepsilon_1' = \varepsilon_0$), $L(\theta,\alpha_p)$ has a single maximum, and as the electrical thickness of the slab increases the second local maximum first appears as a bend in the coefficient and then as an extremum. One can develop a relation for the location of these maxima by setting the θ derivative of $L(\theta,\alpha_p)$ equal to zero, but the resulting equation is complicated and yields little if any physical insight.

Even though the location of α_p does not significantly affect the shape of $L(\theta,\alpha_p)$, α_p has a large effect on its magnitude. Surprisingly, the magnitude of $L(\theta,\alpha_p)$ is much larger for the higher order modes in a given slab than for the lower order modes. For a waveguide one sees the opposite effect--the lowest order modes in a waveguide carry the most energy. Also, one would expect $L(\theta,\alpha_p)$ to have a magnitude of order one, when in, fact, its magnitude can be much larger, especially for the higher order modes. At present an adequate explanation for these effects is not available.

expression similar to the modal launching coefficient and compare the two. This expression, which we call $L^{SDP}(\theta)$, has three forms. These forms, which are comparable to the three forms of $L(\theta,\alpha_p)$, are

$$L^{SDP}(\theta) = \ell(\theta)\cdot\frac{-e^{-H(k_1)}}{2\sqrt{k_1}(\cos\theta + 1)\cos^2(\beta_{21}t)}, \qquad x > 0, \tag{3.8}$$

$$L^{SDP}(\theta) = \ell(\theta)\cdot\frac{j4\sqrt{k_1}\tan[\beta_{21}(\frac{t}{2})]e^{H(k_1)}}{\beta_{21}(\cos\theta - 1)\cos[\beta_{21}(\frac{t}{2})]}, \qquad x < 0, \text{ odd}, \tag{3.9}$$

$$L^{SDP}(\theta) = \ell(\theta)\cdot\frac{j4\sqrt{k_1}\cot[\beta_{21}(\frac{t}{2})]e^{H(k_1)}}{\beta_{21}(\cos\theta - 1)\sin[\beta_{21}(\frac{t}{2})]}, \qquad x < 0, \text{ even}, \tag{3.10}$$

where

$$\ell(\theta) = \frac{k_1\beta_1(k_1\cos\theta)G(k_1\cos\theta,0)e^{j\frac{3}{4}\pi}}{4\pi\sqrt{\pi}\beta_{21}G_-(-k_1\cos\theta)}. \tag{3.11}$$

Figure 3.7 shows $L(\theta,\alpha_p)$ and $L^{SDP}(\theta)$ as functions of θ for a representative case. We note that except near the geometrical optics pole, where $L^{SDP}(\theta)$ is singular, the two functions have the same general shape. They differ greatly in magnitude, but this would be expected. These results support our claim that edge diffraction dominates the mode-launching effect.

The launching coefficients are smooth, slowly varying functions of θ. For a particular choice of slab thickness and permittivity, their

The transverse modal functions also give the expected results. For both surface waves and leaky waves they show the odd or even behavior described previously. If the slab is lossless the transverse variation of a surface wave is strictly sinusoidal and remains essentially sinusoidal for a lossy slab (Figures 3.3, 3.4, and 3.5). Leaky waves exhibit an overall growth in magnitude in the transverse direction away from the screen ($x > 0$) or away from the center of the slab ($x < 0$). Examples of the transverse variation of leaky waves are given in Figures 3.3 and 3.6.

The launching coefficient contains the influence of the excitation on a particular mode. In this respect it is related to diffraction coefficients computed in the geometrical theory of diffraction. We have computed the launching coefficients of contributing modes for several different combinations of slab parameters. From these results we can gain some insight into the factors that influence the launching of guided modes in the slab by the current on the half plane.

The guided wave contributions to $e_z^R(x,y)$ are part of the field diffracted by the screen. The current induced on the half plane excites the slab modes even though the primary field is a plane wave. For the general case of diffraction by a half plane, diffraction from the edge of the half plane has the most influence on the diffracted field. Thus, we might expect that the edge diffraction effect plays the major role in the launching of modes in the slab. Since $e_z^{SDP}(x,y)$ is heavily influenced by the edge diffraction effect, from it we can develop an

zeros of an analytic function in a specified region by dividing the region into a number of subregions and then performing a numerical integration of the function around each subregion. Using the principle of the argument (Hille, 1959b), the routine determined if a zero was located in a particular subregion. If there were one or more zeros in a subregion, the small region provided a good approximate starting place for applying Muller's method. With these poles located it was a simple matter to determine if they were swept in the deformation to SDP^+ or SDP^- and then to compute any resulting contribution to $e_z^R(x,y)$.

3.3 Modal Field Components

With the contributing SWP's and LWP's located, we can compute the launching coefficient, transverse modal function, and propagation factor for a particular pole.

The propagation factor (in eq. 2.69) for a surface wave shows propagation in the positive x direction for $x > 0$ and in the negative x direction for $x < 0$. This is expected since we expect energy to be radiated away from the edge of the half plane. If the slab is lossy the propagation factor shows some decay due to the fact that α_p moves off the vertical line through $\pm\pi/2$ so that $\sin\alpha_p$ becomes complex. For a leaky wave, the propagation factor shows that energy is being radiated away from the edge of the half plane, but it also incorporates a significant amount of decay due to the imaginary part of $\sin\alpha_p$.

$$C(k_x) = \beta_2 \cos(\beta_2 t) + j\beta_1 \sin(\beta_2 t) = 0, \quad \text{odd modes, } x>0, \tag{3.5}$$

$$C(k_x) = \beta_2 \cos[\beta_2(\tfrac{t}{2})] + j\beta_1 \sin[\beta_2(\tfrac{t}{2})] = 0, \quad \text{odd modes, } x<0, \tag{3.6}$$

$$C(k_x) = \beta_1 \cos[\beta_2(\tfrac{t}{2})] + j\beta_2 \sin[\beta_2(\tfrac{t}{2})] = 0, \quad \text{even modes, } x<0. \tag{3.7}$$

By using top sheet values of β_1, we can find the SWP's, and by using bottom sheet values of β_1, we can find the LWP's. For a lossless slab contributing SWP's lie on the segment (k_1,k_2) for $x > 0$ or on the segment $(-k_2,-k_1)$ for $x < 0$ (Coblin 1983). These segments map into the α plane as segments with $u = \pm\pi/2$ and $v \in (0,v_{k2})$ or $v \in (v_{-k2},0)$ for $x > 0$ or $x < 0$, respectively, where v_{kx} is the imaginary part of the mapping of k_x into the α plane (Figures 2.3 and 2.4). If the slab is lossy, the SWP's will still lie on or near these segments. Contributing LWP's lie in the mapping of the fourth quadrant of the bottom sheet, B_4, for $x > 0$ and in the mapping of the second quadrant of the bottom sheet, B_2, for $x <0$ as shown in Figure 2.3. According to Barone (1956) there are an infinite number of LWP's, but only a finite number contribute. This is because the SDP is asymptotic to the boundary between the mappings of the top and bottom sheets (Figure 2.4). Since neither SDP^+ nor SDP^- sweeps the regions B_4 or B_2, respectively, at infinity, not all the LWP's are swept, and only a finite number contribute.

The SWP's and LWP's were found using a numerical search routine developed by Singaraju, Giri, and Baum (1976). This routine found the

Under the screen the SWP's and LWP's are zeros of

$$C'(k_x) = (\beta_1 - \beta_2)e^{-j\beta_2 t} - (\beta_1 + \beta_2)e^{+j\beta_2 t}, \quad x > 0. \tag{3.3}$$

In this case $C'(k_x)$ is, within a factor, simply the numerator of $G(k_x,0)$. Thus, the poles of G/G_+ for $x > 0$ are the same as the zeros of $G(k_x,0)$, validating our claim that the slab shows the characteristics of a grounded dielectric slab waveguide for $x > 0$. For $x < 0$ the SWP's and LWP's are the zeros of

$$\begin{aligned} C'(k_x) &= (\beta_1 - \beta_2)^2 e^{-j\beta_2 t} - (\beta_1 + \beta_2)^2 e^{+j\beta_2 t} \\ &= \left[(\beta_1 - \beta_2)e^{-j\beta_2(\frac{t}{2})} - (\beta_1 + \beta_2)e^{+j\beta_2(\frac{t}{2})}\right] \cdot \\ &\quad \left[(\beta_1 - \beta_2)e^{-j\beta_2(\frac{t}{2})} + (\beta_1 + \beta_2)e^{+j\beta_2(\frac{t}{2})}\right], \quad x < 0. \end{aligned} \tag{3.4}$$

In this case $C'(k_x)$ is, within a factor, the denominator of $G(k_x,0)$. Thus, the poles of G/G_+ for $x < 0$ are the same as the poles of $G(k_x,0)$, that is, the slab shows the characteristics of a dielectric slab waveguide in space for this region.

From the expression for $C'(k_x)$ we can develop a set of characteristic equations for each case (i.e., modes odd with respect to the half plane for $x > 0$, modes odd with respect to the center of the slab for $x < 0$, and modes even with respect to the center of the slab for $x < 0$). These characteristic equations can be written as

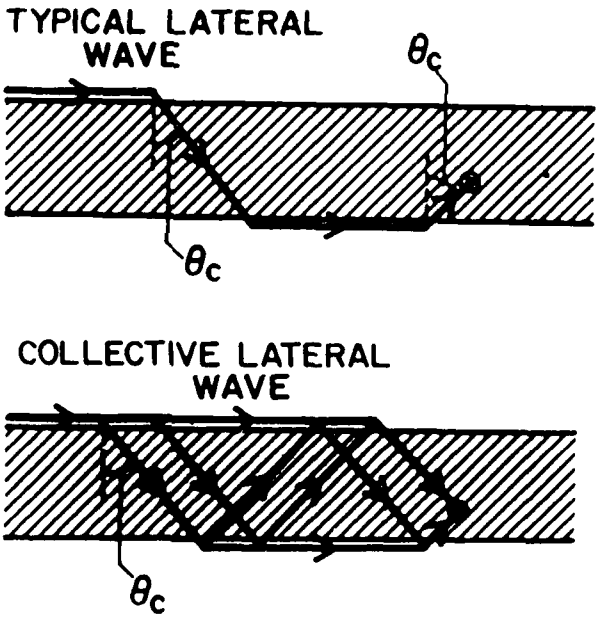

Figure 2.5. Diagrams of lateral wave ray paths (after Tamir and Felsen, 1965).

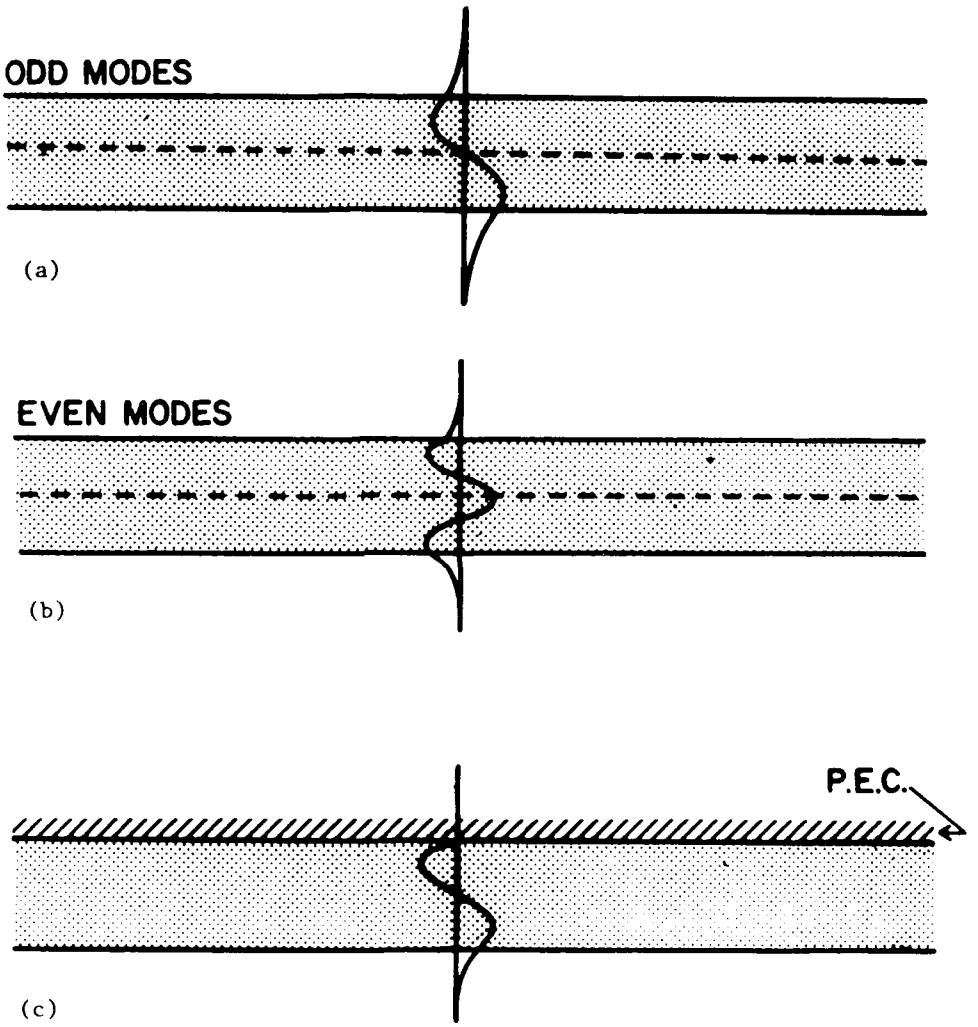

Figure 3.1. Generic field distributions for dielectric slab waveguides: (a) odd modes for open slab, (b) even modes for open slab, (c) "grounded-slab" mode under p.e.c.

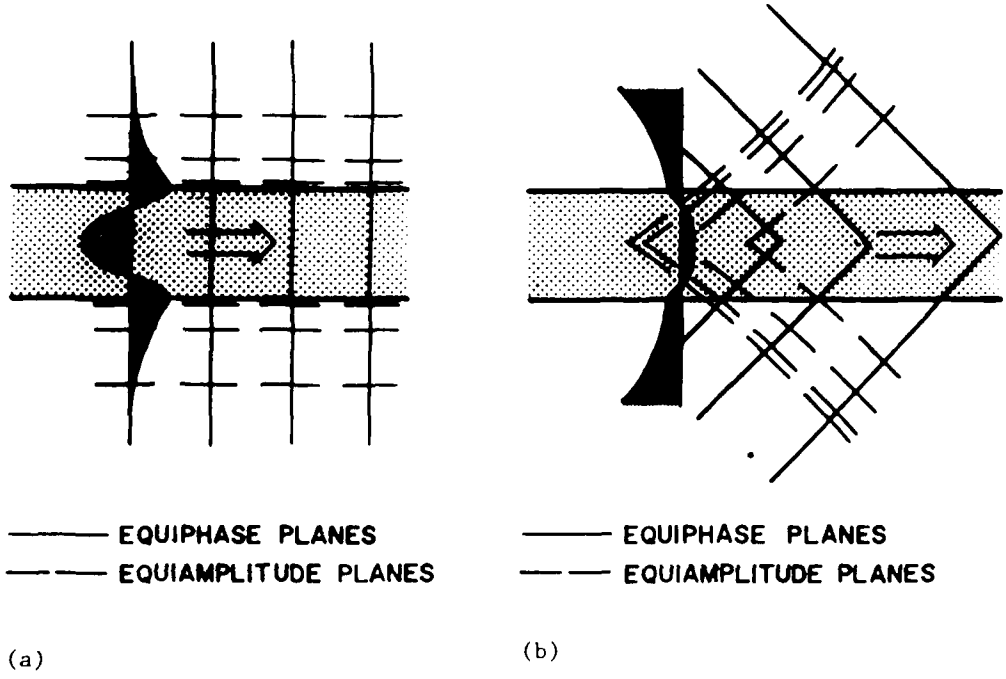

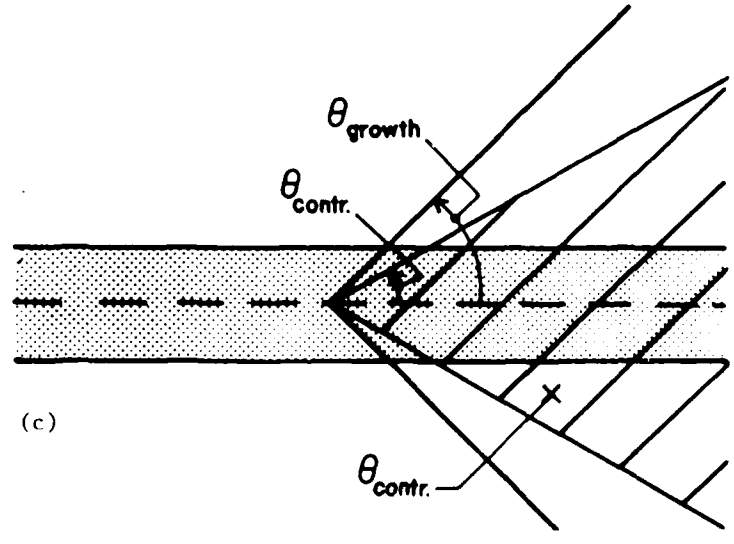

Figure 3.2. Surface and leaky waves: (a) surface wave, (b) leaky wave, (c) region of contribution for a leaky wave.

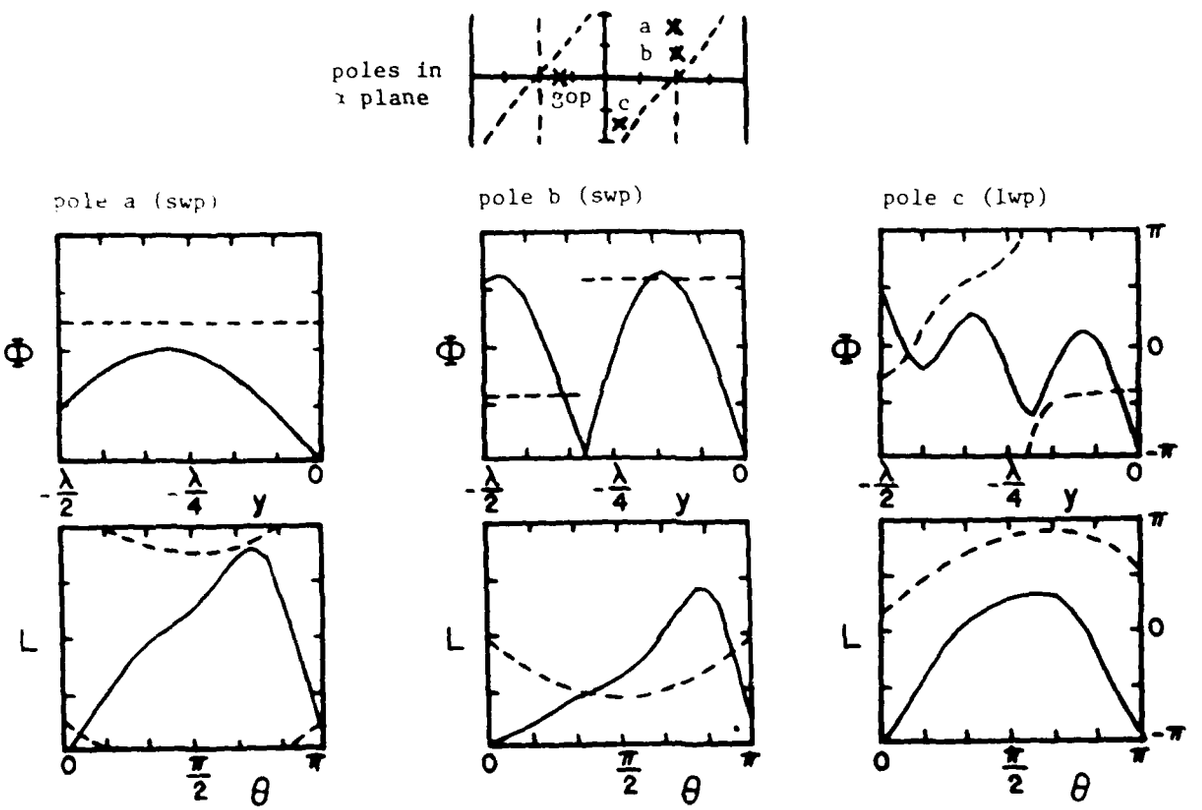

Figure 3.3. Φ and L for contributing modes in a slab with $\epsilon_2' = 4\epsilon_0$, $t' = \lambda_0/4$, $x > 0$.

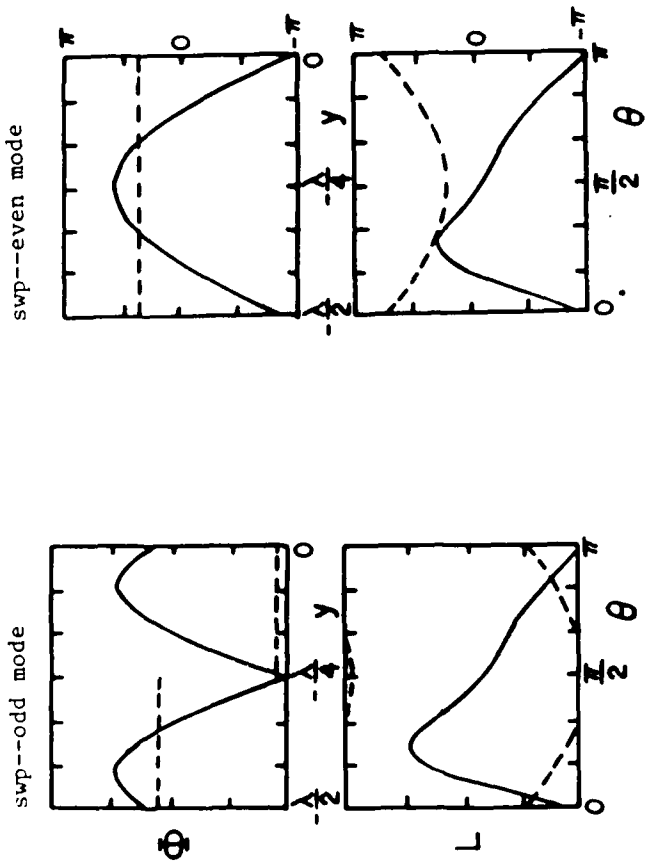

Figure 3.4. ψ and L for contributing modes in a slab with $\varepsilon_2' = 4\varepsilon_0$, $t' = \lambda_0/4$, $x < 0$.

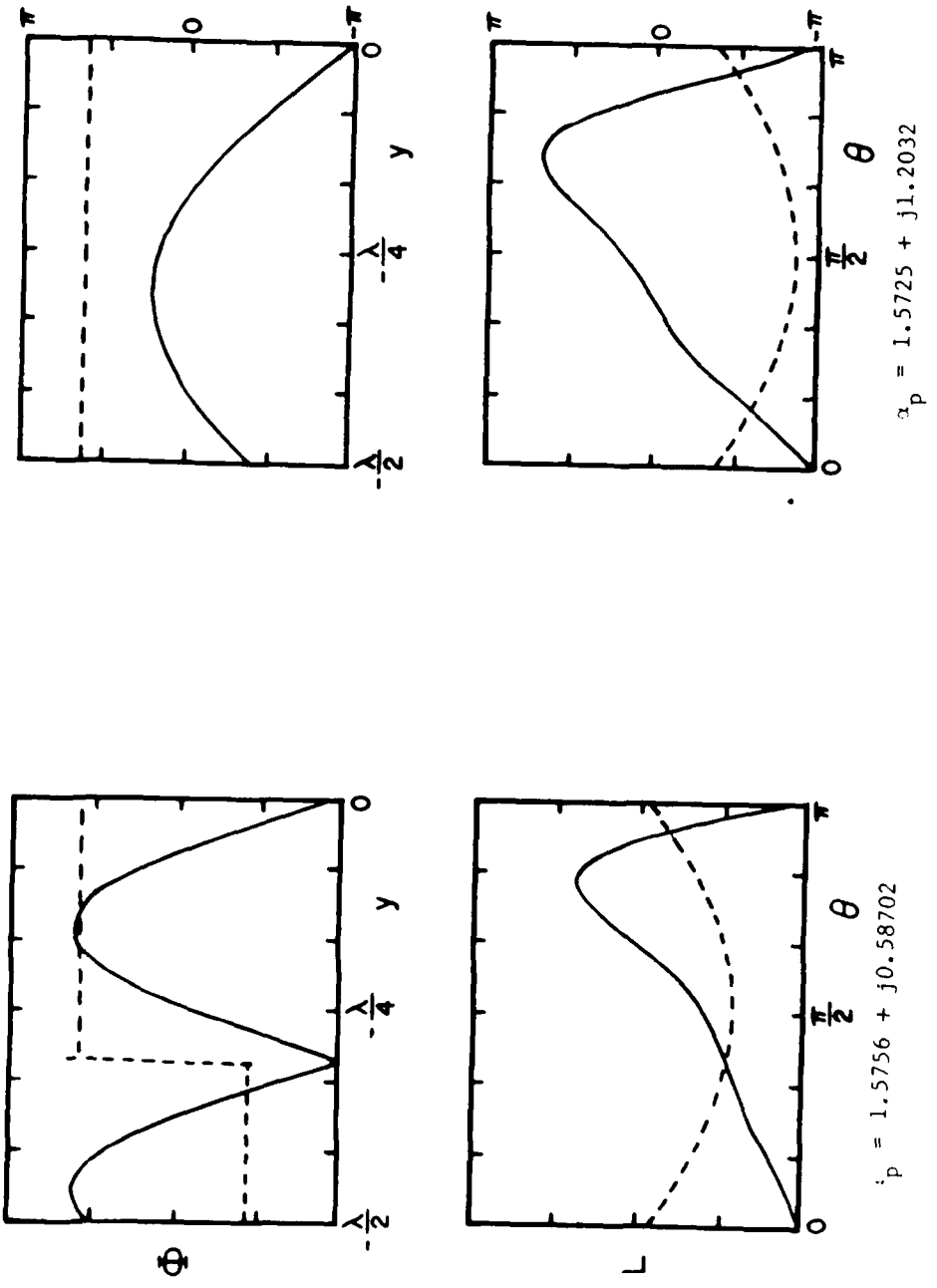

α_p = 1.5725 + j1.2032

α_p = 1.5756 + j0.58702

Figure 3.5. Θ and L for surface waves in a lossy slab with $\varepsilon_2' = (4 - j0.01)\varepsilon_0$, $t' = \lambda_0/2$, $x > 0$.

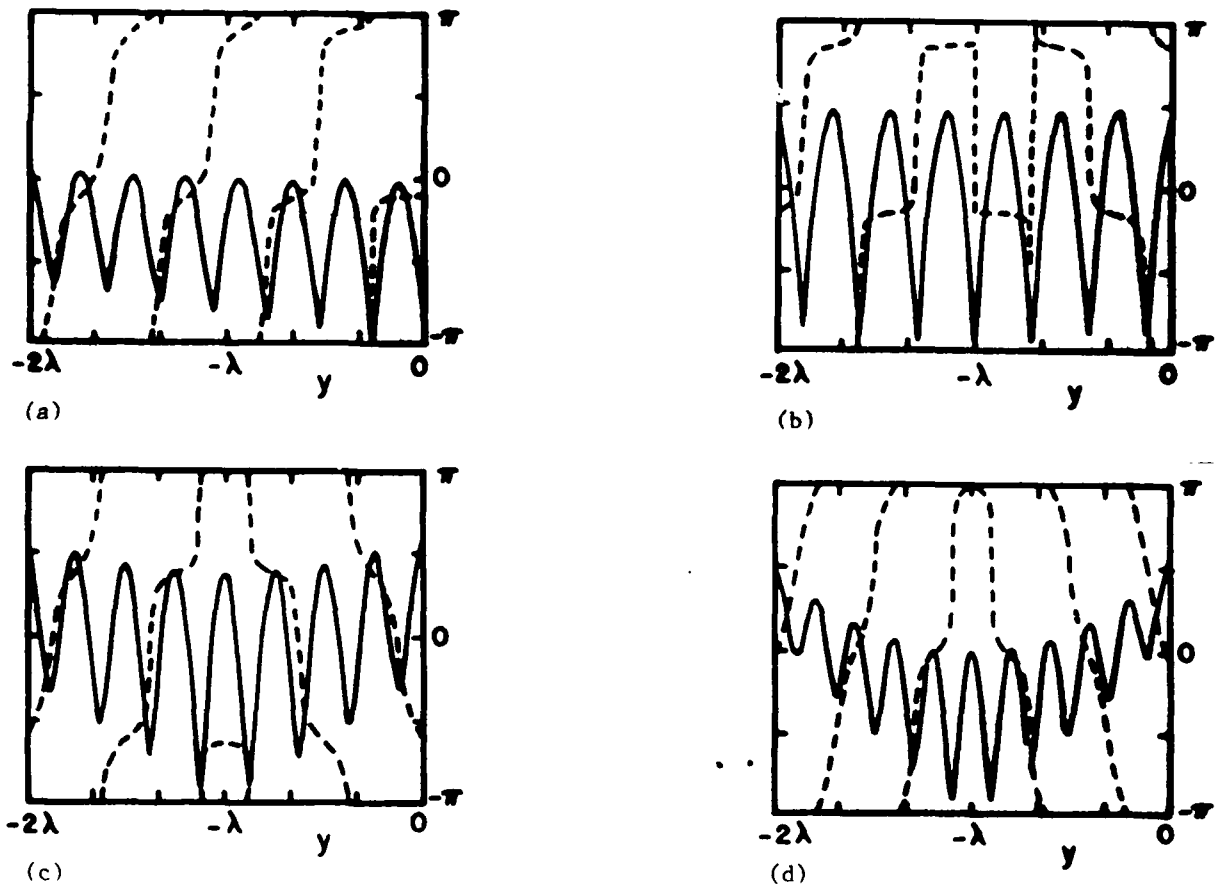

Figure 3.6. Φ for contributing leaky waves in a slab with $\varepsilon_2' = 4\varepsilon_0$, $t' = 2\lambda_0$:
(a) $\alpha_p = 0.784 - j0.118$, $x > 0$, (b) $\alpha_p = -1.34 + j0.162$, $x < 0$,
(c) $\alpha_p = -0.432 + j0.405$, $x < 0$, (d) $\alpha_p = -0.134 + j1.25$, $x < 0$.

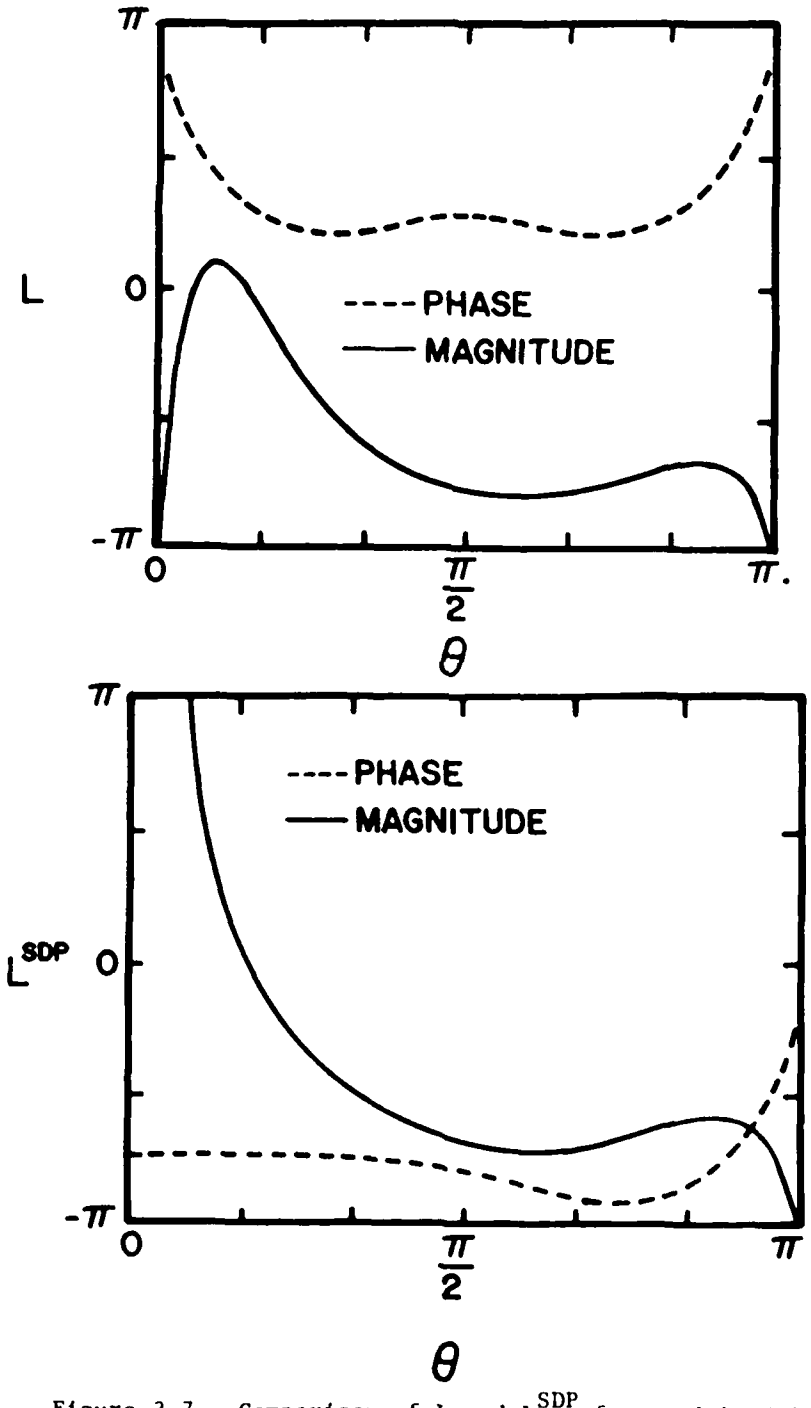

Figure 3.7. Comparison of L and L^{SDP} for a slab with $\epsilon_2' = 4\epsilon_0$, $t' = 0.85\lambda_0$ (odd modes for $x < 0$).

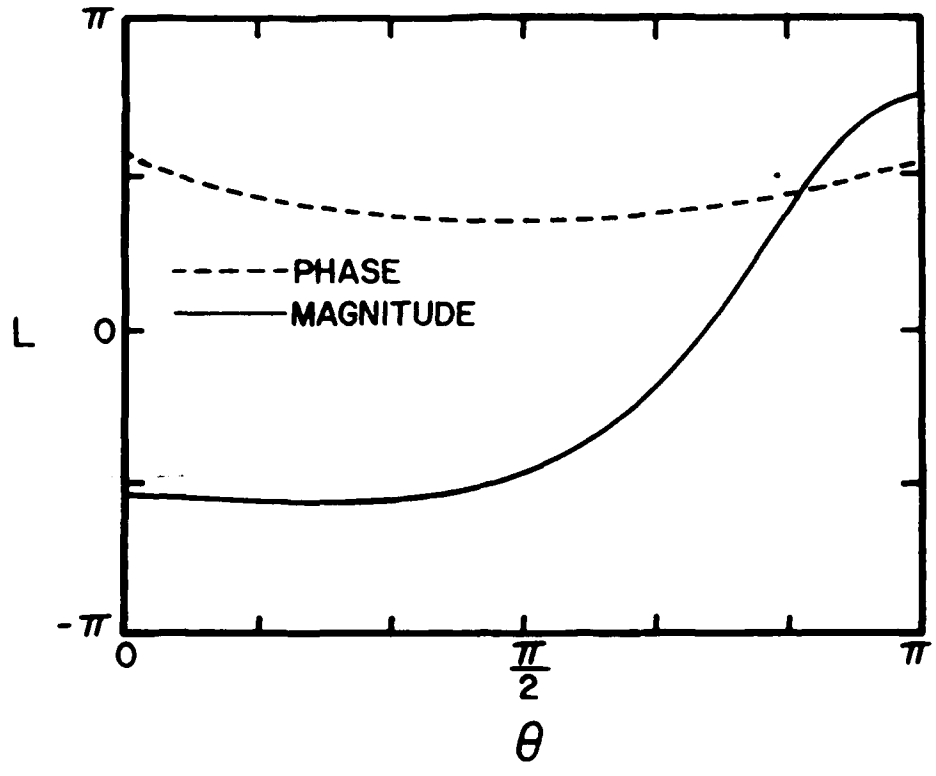

Figure 3.8. Representative launching coefficients for a slab with $\epsilon_2' = 10\epsilon_0$, $t' = \lambda_0/2$ showing nonzero behavior at $\theta = 0^\circ$ and $\theta = 180^\circ$.

BIBLIOGRAPHY

Barone, S. (1956), "Leaky Wave Contributions to the Field of a Line Source above a Dielectric Slab", Microwave Res. Inst., Polytechnic Inst. of Brooklyn, Report R-532-56, PIB-462, November 1956.

Coblin, R.D. (1983), "Scattering of an Electromagnetic Plane Wave from a Perfectly Electrically Conducting Half-plane in the Proximity of Planar Media Discontinuities", Ph. D. dissertation, University of Mississippi, February 1983.

Felsen, L.B.; N. Marcuvitz (1973a), Radiation and Scattering of Waves. Englewood Cliffs, N.J.: Prentice-Hall, pp. 278-284.

Felsen, L.B.; N. Marcuvitz (1973b), op. cit., pp. 377-399.

Felsen, L.B.; N. Marcuvitz (1973c), op. cit., pp. 399-410.

Harrington, R.F. (1961), Time-Harmonic Electromagnetic Fields. New York: McGraw-Hill.

Heitman, W.G.; P.M. van den Berg (1975), "Diffraction of Electromagnetic Waves by a Semi-infinite Screen in Layered Medium", Can. J. Phys., 53(14), pp. 1305-1317.

Hessel, A. (1969a), "General Characteristics of Traveling-wave Antennas", in Collin, R.E.; F.J. Zucker, Antenna Theory. New York: McGraw-Hill, 1969, pp. 151-258.

Hessel, A. (1969b), op. cit., pp 166-181.

Hessel, A. (1969c), op. cit., pp 165-180.

Hille, E. (1959a), Analytic Function Theory, Vol. 1. New York: Chelsea, pp. 203-204.

Hille, E. (1959b), op. cit., p. 253.

Mittra, R.; S.W. Lee (1971a), Analytic Techniques in the Theory of Guided Waves. New York: Macmillan, pp. 73-153.

Mittra, R. and S.W. Lee (1971b), op. cit., pp. 23-29.

Singaraju B.D.; D.V. Giri; C.E. Baum (1976), "Further Developments in the Application of Contour Integration to the Evaluation of the Zeros of Analytic Functions and Relevant Computer Programs", Air Force Weapons Lab., Mathematical Notes, Note 42, March 1976.

Tamir, T.; L.B. Felsen (1965a), "On Lateral Waves in Slab Configurations and Their Relation to Other Wave Types", IEEE Trans. Antennas Propagat., AP-13, pp. 410-422.

Tamir, T.; L.B. Felsen (1965b), op. cit., pp. 419-422.

END

DATE
FILMED
7-85

DTIC